

miR-3613-3p/MAP3K2/p38/caspase-3 pathway regulates the heat-stress-induced apoptosis of endothelial cells

JIE LIU¹, SIYA XU², SHIXIN LIU² and BINGGUAN CHEN³

¹Department of Intensive Care Unit, Hefei Boe Hospital Co., Ltd., Hefei, Anhui 230011;

²Department of Emergency, Central Theater General Hospital of The People's Liberation Army of China, Wuhan, Hubei 430070; ³Department of General Surgery, Hefei Boe Hospital Co., Ltd., Hefei, Anhui 230011, P.R. China

Received December 4, 2020; Accepted May 11, 2021

DOI: 10.3892/mmr.2021.12272

Abstract. Previous studies have identified microRNA (miRNA/miR)-3613-3p as a heat stress (HS)-related miRNA in endothelial cells that can lead to apoptosis. However, the mechanism underlying the miR-3613-3p-mediated apoptosis of HS-exposed endothelial cells remains unclear. In the present study, western blot analysis and reverse transcription-quantitative PCR were used to determine protein and miRNA expression levels, respectively. Annexin V-fluorescein isothiocyanate/propidium iodide staining, caspase-3 activity measurements and DNA fragmentation assays were performed to detect apoptosis. To evaluate whether mitogen-activated protein kinase kinase 2 (MAP3K2) was a direct target of miR-3613-3p, a luciferase reporter assay was performed. In addition, transient transfection was used to carry out loss- and gain-of-function experiments. The results revealed that miR-3613-3p expression was reduced in human umbilical vein endothelial cells (HUVECs) following HS, which led to apoptosis. Mechanistically, following HS, a decrease in miR-3613-3p binding to the 3'-untranslated region of MAP3K2 directly upregulated its expression, and the downstream p38 and caspase-3 pathways, thereby leading to apoptosis. Taken together, the results of the present study demonstrated that HS suppressed miR-3613-3p expression, which activated the MAP3K2/p38/caspase-3 pathway, leading to the apoptosis of HUVECs. In conclusion, the miR-3613-3p/MAP3K2/p38/caspase-3 pathway may

serve an indispensable role in regulating the progression of apoptosis, indicating a regulatory role of miR-3613-3p in the pathophysiology of HS-exposed endothelial cells.

Introduction

Heat stroke, which has a mortality rate of 10-15% worldwide (1), arises from acute and irreversible multiple organ dysfunction induced by severe heat stress (HS) (2). Severe HS-induced multiple organ dysfunction is thought to be associated with excessive death of endothelial cells (e.g., via apoptosis, autophagy or necrosis), which constitute the greatest surface area of the human circulatory system (3-5). Notably, HS can cause damage to cells in various tissues, including endothelial cells. In response to the direct injurious effect of HS and the increased levels of inflammatory mediators caused by HS, endothelial cell apoptosis is an early event in heat stroke, suggesting its critical role in the pathogenesis of this condition (2,3,6). Endothelial cell apoptosis is closely associated with microvascular dysfunction, including impaired permeability, coagulation, fibrinolysis, vascular tone and leukocyte recruitment (7). Microvascular dysfunction causes interstitial leakage, impaired microcirculatory blood flow and tissue hypoperfusion, and directly contributes to life-threatening organ failure (8-10). A more detailed understanding of HS-induced endothelial cell apoptosis may be helpful for future therapy and in limiting HS-induced organ failure.

MicroRNA (miRNA/miR) is a type of endogenous small noncoding RNA molecules that regulate gene expression by pairing with a sequence-specific target or via other mechanisms; therefore, it has been suggested that miRNAs can control diverse cellular and signalling pathways (11). In numerous pathological conditions, miRNA and miRNA-related regulatory networks serve a crucial role in the prevention and treatment of endothelial cell death (11-14). Several miRNA molecules have been reported to be aberrantly expressed in endothelial cells following HS, and their dysregulation is thought to be linked to pathological phenotypes of endothelial cells, such as proapoptotic, proinflammatory, proadhesive and procoagulant phenotypes (12). However, despite extensive investigation of these molecules in other diseases, exploration of their roles and the underlying pathogenic mechanisms in HS-induced endothelial cell death is limited.

Correspondence to: Dr Bingguan Chen, Department of General Surgery, Hefei Boe Hospital Co., Ltd., 01 Intersection of Dongfang Avenue and Wenzhong Road, Xinzhan, Hefei, Anhui 230011, P.R. China
E-mail: chenbingguan2020@163.com

Abbreviations: miR-3613-3p, microRNA-3613-3p; HS, heat stress; MAP3K2, mitogen-activated protein kinase kinase 2; HUVEC, human umbilical vein endothelial cell; 3'-UTR, 3'-untranslated region; MAPK, mitogen-activated protein kinase

Key words: heat stress, apoptosis, endothelial cell

In endothelial cells, the mitogen-activated protein kinase (MAPK) pathway is reported to be one of the most frequently activated pathways in several pathogenic conditions (13,14). Accumulating evidence has indicated that the MAPK pathway is involved in HS-induced organ injury and endothelial cell apoptosis; therefore, this pathway is thought to be a valuable therapeutic target in heat stroke (15). Several miRNA molecules, such as miR-199b-3p, miR-30-3p and miR-9-5p in endothelial cells, have been proposed to negatively regulate the MAPK pathway and inhibit endothelial cell apoptosis (16-18). However, whether MAPK can be negatively regulated by relevant miRNAs in endothelial cells after HS and its role remains poorly understood.

Our previous study demonstrated that miR-3613-3p was suppressed in HS-treated human umbilical vein endothelial cells (HUVECs) (19). In our preliminary study, it was revealed that a decrease in miR-3613-3p might promote cell apoptosis by negative post-transcriptional regulation of the target gene MAPK kinase kinase 2 (MAP3K2) (19), a component of the MAPK pathway. However, whether the miR-3613-3p/MAP3K2 axis, along with downstream signalling molecules, contributes to HS-induced apoptosis remains unclear.

The aim of the present study was to investigate whether miR-3613-3p is a critical mediator in the progression of the HS-induced apoptosis of HUVECs, and whether this may involve changes in the activity of MAP3K2 and its downstream molecules.

Materials and methods

Cell culture and treatment. HUVECs were purchased from the American Type Culture Collection and cultured in RPMI-1640 medium (Invitrogen; Thermo Fisher Scientific, Inc.) supplemented with 5% FBS (Invitrogen; Thermo Fisher Scientific, Inc.), 1% Eco Growth Supplement (Promocell GmbH), 100 U/ml penicillin and 100 µg/ml streptomycin (Invitrogen; Thermo Fisher Scientific, Inc.) in a humidified atmosphere at 37°C and 5% CO₂. All experiments were carried out with the 3-6 generation HUVECs. For induction of HS, HUVECs were heated in a humidified incubator at different temperatures (39, 41, 43 or 45°C for 2 h followed by 37°C for 6 h) or for different heat exposure times (43°C for 1, 2, 3 or 4 h followed by 37°C for 6 h), then transferred to normal culture conditions (5% CO₂ at 37°C) for 6 h before analysis. Cells cultured at 37±0.5°C for 2 h were used as control cells. The use of non-immortal HUVECs has received ethical approval from the Ethics Committee of Hefei Boe Hospital Co., Ltd. (approval no. 20190106).

Transient transfection. The miR-3613-3p mimic (cat. no. miR10017991-1-5, https://www.ribobio.com/en/product_detail/?sku=miR10017991-1-5), negative control (NC) miRNA (miR-NC; cat. no. miR1N0000001-1-5, <https://www.ribobio.com/en/product-search/?Category=all&species=all&keywords=micron mimic NC>), miR-36-13-3p inhibitor (cat. no. miR20017991-1-5, https://www.ribobio.com/en/product_detail/?sku=miR20017991-1-5) and anti-miR-NC (cat. no. miR2N0000001-1-5, <https://www.ribobio.com/en/product-search/?category=all&species=all&keywords=micrOFF inhibitor NC#22>) were purchased from

Guangzhou RiboBio Co., Ltd.. For construction of recombinant DNA or interference with gene expression, the pcDNA3.1 plasmid (cat. no. E0648; Sigma-Aldrich; Merck KGaA) was used as the vector. The pcDNA3.1-MAP3K2 plasmid was constructed by Shanghai GeneChem Co., Ltd.. The empty pcDNA3.1 vector was used as the control. The MAP3K2 small interfering RNA (siRNA; si-MAP3K2; cat. no. siB06111516204-1-5) and corresponding NC (si-NC; cat. no. siN0000001-1-5) were purchased from Guangzhou RiboBio Co., Ltd.. Cells were seeded into 6-well plates at a density of ~1.5×10⁵ cells/well. Following the manufacturer's instructions, transient transfection was carried out with Lipofectamine® 3000 reagent (Invitrogen; Thermo Fisher Scientific, Inc.) at 37°C for 24 h. Different concentrations of miR-3613-3p mimic or miR-3613-3p inhibitor were used (miR-3613-3p mimic at 25, 50 and 100 nM; miR-3613-3p inhibitor at 25, 50 and 100 nM) to determine the effect of HS on apoptosis of HUVECs. The appropriate concentrations of these factors were selected and used in further experiments. The concentrations of other reagents were as follows: miR-NC, 50 nM; anti-miR-NC, 100 nM; pcDNA3.1-MAP3K2, 100 nM; pcDNA3.1, 100 nM; si-MAP3K2, 50 nM; and si-NC, 50 nM. After transfection, cells were treated with 43°C or control heat treatments. Then, transfected cells were collected for subsequent analysis.

RNA extraction and reverse transcription-quantitative PCR (RT-qPCR). Total RNA was isolated from HUVECs (~5×10⁶ cells) using TRIzol® (Thermo Fisher Scientific, Inc.) and the miRNA easy mini kit (Qiagen, Inc.), according to the manufacturer's protocols. A Nanodrop™ spectrophotometer (Thermo Fisher Scientific, Inc.) was used to measure the quantity and quality of RNA, and 1% agarose gel electrophoresis was used to detect RNA integrity. The expression levels of miRNA were detected via RT-qPCR, and the primers were synthesized and purchased from Shanghai Gene Pharmaceutical Co., Ltd. U6 was employed as the endogenous control for miRNA expression. The primer sequences were as follows: miR-3613-3p sense, 5'-CGTCCCTTCCCAACCCGAAAAAAA-3' and antisense, 5'-CGCAGGGTCCGAGGTATTC-3'; and U6 sense, 5'-CTCGCTTCGGCAGCACAC-3' and antisense, 5'-AACGCTTCACGAATTTGCGT-3'. Briefly, specific stem-loop primers and a TaqMan® MicroRNA Reverse Transcription kit (Applied Biosystems; Thermo Fisher Scientific, Inc.) were used to reverse transcribed sample total RNA (10 ng) into cDNA. In a 15-µl reaction volume, mixtures were incubated for 30 min at 16°C, 30 min at 42°C and 5 min at 85°C, and held at 4°C. Following the RT reaction, qPCR was carried out with an ABI 7300 Real-Time PCR system (Bio-Rad Laboratories, Inc.) and SYBR Green (Invitrogen; Thermo Fisher Scientific, Inc.) according to the manufacturer's protocol. The thermocycling conditions were 95°C for 10 min, followed by 40 cycles of 95°C for 15 sec and 60°C for 60 sec in a 20-µl reaction volume (20,21). The relative level of each miRNA was determined by the 2^{-ΔΔCq} method (22). All results were normalized to U6 expression levels, which were analyzed simultaneously. All experiments were performed at least in triplicate.

Flow cytometric analysis of apoptosis. Cell apoptosis was determined with an Annexin V-FITC Apoptosis kit

(Invitrogen; Thermo Fisher Scientific, Inc.) according to the manufacturer's protocol. In total, $\sim 1 \times 10^6$ cells were collected, washed with ice-cold PBS prior to resuspension in binding buffer containing 5 μ l Annexin V-FITC for 10 min in the dark at room temperature. Subsequently, the cells were pelleted by centrifugation at $\sim 157 \times g$ and 4°C for 10 min, the buffer was removed and the cells were resuspended in reaction buffer containing 10 μ l propidium iodide (PI). The suspension was mixed and incubated in the dark at room temperature for 15 min. Finally, cell apoptotic rates (early+late) were determined using a flow cytometer (FACSCanto™ II; BD Biosciences). FlowJo version 7.6.1 software (Tree Star, Inc.) was used to analyze the data. The experiment was performed at least three times.

Protein extraction and western blot analysis. Protein extraction, measurement of total protein concentration and western blot analysis were performed as described previously (19). The primary antibodies used were as follows: Mouse anti-human MAP3K2 (cat. no. SAB5300054), mouse anti-human p38 MAPK (cat. no. M8177), mouse anti-human phosphorylated (p)-p38 MAPK (cat. no. MABS64), mouse anti-human extracellular signal-regulated kinase (ERK1/2; cat. no. M8159), mouse anti-human p-ERK1/2 (cat. no. M7802), mouse anti-human c-Jun N-terminal kinase (JNK; cat. no. SAB4200176), rabbit anti-human p-JNK (cat. no. ZRB1173), mouse anti-human caspase-3 (cat. no. C5737) and mouse anti-human actin (cat. no. A4700) (all from Sigma-Aldrich; Merck KGaA). All primary antibodies were diluted 1:1,000. Goat anti-mouse horseradish peroxidase-conjugated immunoglobulin G (cat. no. SAB3701029) and goat anti-rabbit horseradish peroxidase-conjugated immunoglobulin G (cat. no. AP156P) (both from Sigma-Aldrich; Merck KGaA) were diluted 1:8,000 and used as secondary antibodies. Protein expression levels were normalized to those of actin as the endogenous control.

Luciferase reporter assay. The luciferase vector reporter plasmids pGL3-MAP3K2 with the wild-type 3'-untranslated region (3'-UTR) (MAP3K2-WT) or mutant 3'-UTR (MAP3K2-MUT) were purchased from Guangzhou RiboBio Co., Ltd. miR-NC or anti-miR-NC were used as the NCs. HUVECs ($\sim 1 \times 10^5$ cells/well) were seeded in 24-well plates and cultured for 24 h prior to transfection. Cells were co-transfected with luciferase vectors (MAP3K2-WT or MAP3K2-MUT reporter plasmid) and either miR-3613-3p mimic or miR-NC at room temperature for 24 h. Simultaneously, cells were co-transfected with luciferase vectors (MAP3K2-WT or MAP3K2-MUT reporter plasmid) and either miR-3613-3p inhibitor or anti-miR-NC at room temperature for 24 h. Lipofectamine® 3000 reagent was used according to the manufacturer's protocol. The dual-luciferase activity was measured at 48 h after transfection. The dual-Luciferase reporter system (Promega Corporation) was used to quantify Firefly and Renilla luciferase activities according to manufacturer's protocol. All experiments were performed in triplicate; n=3-6 for each experiment. The final concentrations were as follows: MAP3K2-WT, 100 nM; MAP3K2-MUT, 100 nM; miR-3613-3p mimic, 50 nM; miR-3613-3p inhibitor, 100 nM;

miR-NC, 50 nM; and anti-miR-NC, 100 nM. All experiments were performed in triplicate; n=3-6 for each experiment.

Treatments with selective pathway inhibitors. SB203580 (an inhibitor of p38 MAPK), PD98059 (an inhibitor of ERK) and SP600125 (an inhibitor of JNK) were from Sigma-Aldrich (Merck KGaA). All inhibitors were diluted in DMSO (stock concentrations 10 and 20 mM) and kept at -20°C. During the experiments, they were used at a final concentration of 10 μ M. They were respectively added in culture medium 24 h prior to HS exposure at 37°C.

Caspase-3 activity assay. A caspase-3 activity fluorescent assay kit (Enzo Life Sciences, Inc.) was used according to the manufacturer's protocol. Cells were seeded at a density of 1×10^5 cells/well in 96-well plates. After 24 h, cells were exposed to HS or control heat. Cells were then lysed in caspase-3 sample lysis buffer, and total cellular protein was extracted and quantified using a BCA Protein assay kit (Thermo Fisher Scientific, Inc.) according to the manufacturer's protocol. Prior to the caspase-3 assay, samples containing equal amounts of total protein were incubated with the DEVD substrate conjugate provided in the kit at 37°C for 2 h. The samples were then evaluated by measurement at an excitation wavelength of 400 nm and emission wavelength of 505 nm in an automatic microplate reader (SpectraMax M5; Molecular Devices, LLC).

DNA fragmentation assay. A Cellular DNA Fragmentation ELISA kit (Roche Applied Science; cat. no. 11585045001) was used according to the manufacturer's instructions. This assay is based on the quantitative detection of 5-bromo-2'-deoxyuridine (BrdU)-labeled DNA fragments. Cells were seeded at a density of 1×10^5 cells/well in 96-well plates. After 24 h of growth, cells were exposed to different treatments. Subsequently, 10 μ M BrdU was added to each well, and the cells were cultured with BrdU for 24 h. The complexes were centrifuged at $\sim 250 \times g$ for 10 min at 4°C, the supernatant carefully removed. After DNA labelling, the cells were lysed in 200 μ l incubation buffer and soluble DNA fragments were quantified using the Cellular DNA Fragmentation ELISA kit, according to the manufacturer's instructions. Absorbance values were detected spectrophotometrically at 450 nm using an ELx808 ELISA reader (BioTek Instruments). All experiments were performed in triplicate.

Statistical analysis. Data are presented as the mean \pm standard error of the mean from at least three independent experiments performed in duplicate. Statistical analysis was performed using SPSS version 20.0 (IBM Corp.). Differences between two groups were compared using unpaired Student's t-test. Comparisons among multiple groups were performed with one-way analysis of variance followed by Tukey's test. $P < 0.05$ was considered to indicate a statistically significant difference.

Results

Apoptosis is induced by HS in HUVECs. To evaluate the apoptosis of HUVECs following HS, Annexin V-fluorescein isothiocyanate/PI staining and flow cytometry were performed.

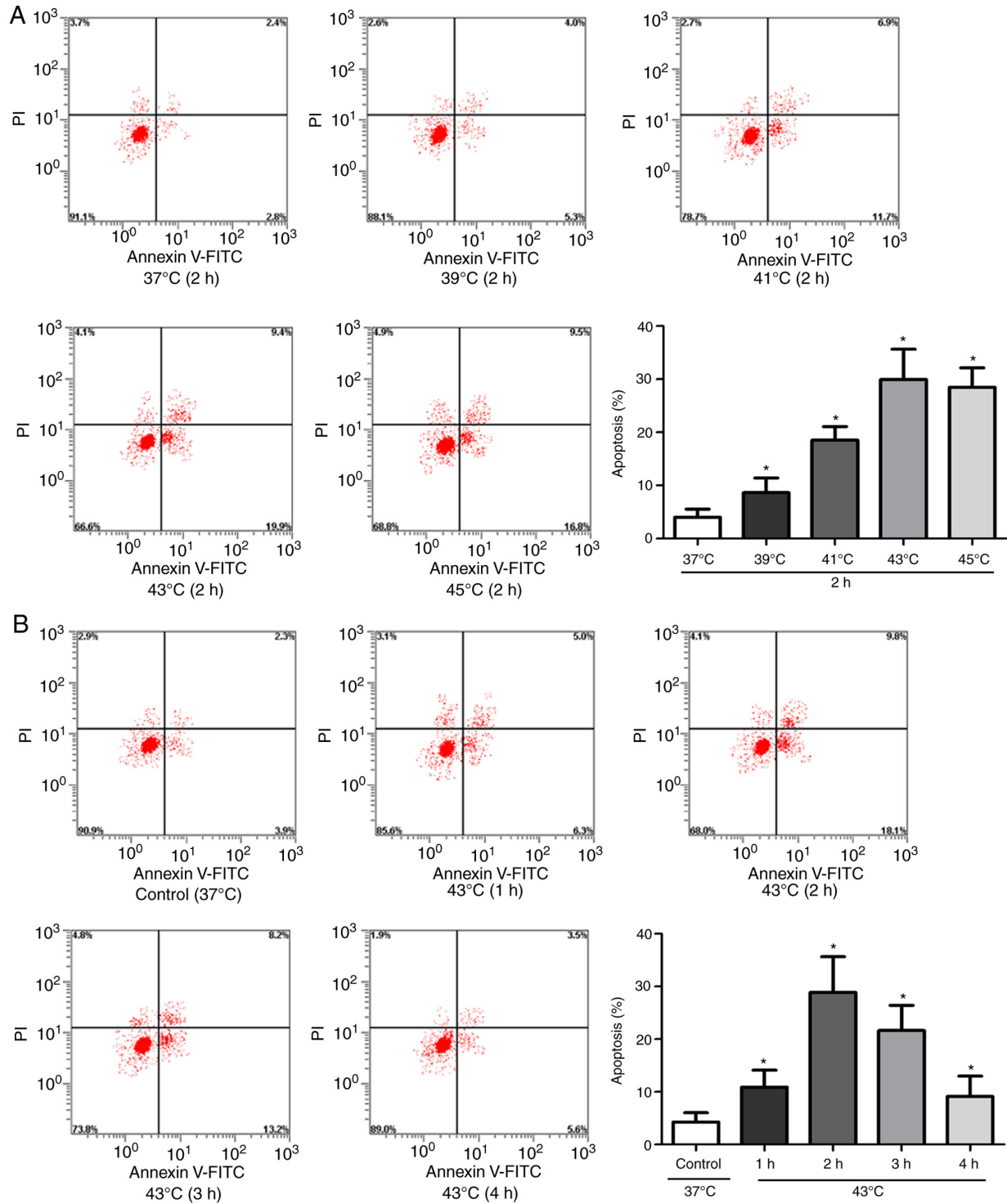


Figure 1. Apoptosis is induced by HS in HUVECs. (A) Apoptosis of HUVECs after HS exposure at different temperatures was determined using an Annexin V/PI apoptosis kit. (B) Apoptosis of HUVECs after HS exposure for different durations was determined with an Annexin V/PI apoptosis kit. * $P < 0.05$ vs. 37°C group. FITC, fluorescein isothiocyanate; HUVECs, human umbilical vein endothelial cells; HS, heat stress; miR-3613-3p, microRNA-3613-3p; PI, propidium iodide.

Cells were incubated at different temperatures (39, 41, 43, or 45°C for 2 h followed by 37°C for 6 h) or for different heat exposure times (43°C for 1, 2, 3 or 4 h followed by 37°C for 6 h). The apoptotic rate was increased with increasing temperature or heat exposure time, peaking at 43°C or 2 h in the respective experiments (Fig. 1A and B). These results suggested that HUVEC apoptosis was enhanced by HS.

HS induces miR-3613-3p downregulation and MAP3K2 upregulation in HUVECs. To evaluate the expression levels of miR-3613-3p and MAP3K2 in HUVECs during HS exposure, RT-qPCR and western blot analysis were performed. In HUVECs treated with different temperatures or for different heat exposure durations, the expression levels of miR-3613-3p were decreased, whereas those of MAP3K2 were increased. As

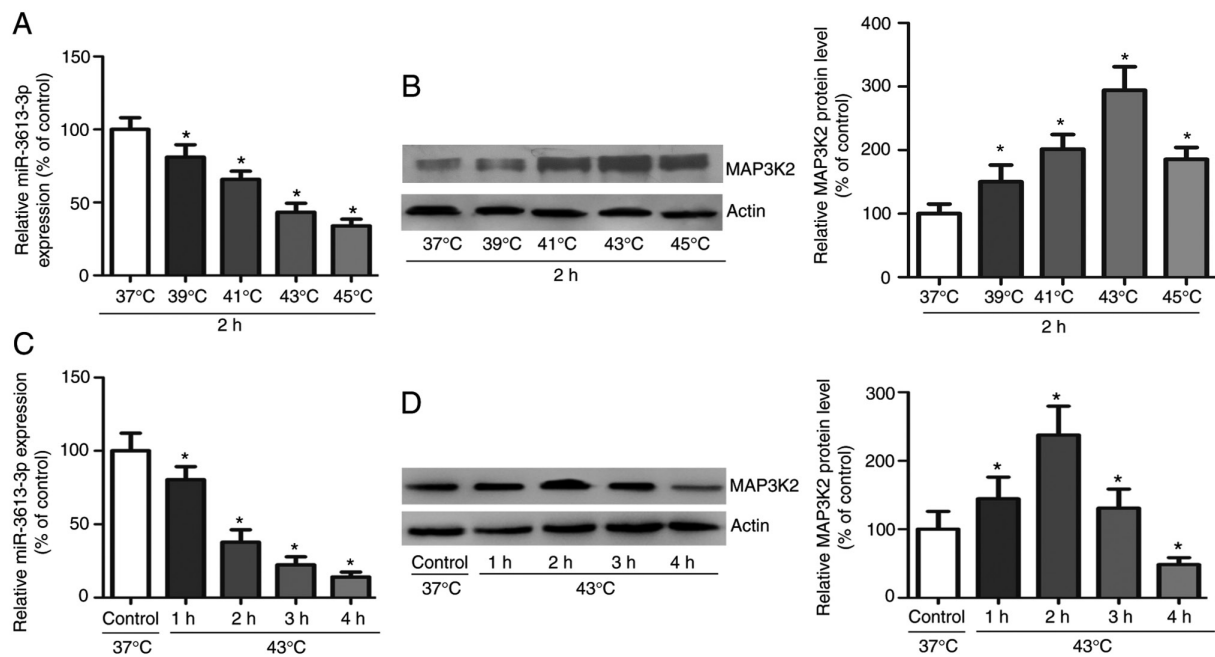


Figure 2. HS induces miR-3613-3p downregulation and MAP3K2 upregulation in HUVECs. (A) Expression of miR-3613-3p in HUVECs after HS exposure at different temperatures was determined by RT-qPCR. (B) Expression of MAP3K2 in HUVECs after HS exposure at different temperatures was determined by western blot analysis. (C) Expression of miR-3613-3p in HUVECs after HS exposure for different durations was determined by RT-qPCR. (D) Expression of MAP3K2 in HUVECs after HS exposure for different durations was determined by western blot analysis. * $P < 0.05$ vs. 37°C group. HUVECs, human umbilical vein endothelial cells; HS, heat stress; miR-3613-3p, microRNA-3613-3p; MAP3K2, mitogen-activated protein kinase kinase 2; RT-qPCR, reverse transcription-quantitative PCR.

shown in Fig. 2A and B, the expression levels of miR-3613-3p were significantly decreased and those of MAP3K2 were significantly increased at all time points. Furthermore, as shown in Fig. 2C and D, the expression levels of miR-3613-3p were consistently decreased at all durations, and those of MAP3K2 were significantly increased after HUVECs were exposed to HS for 2 h. These results indicated that HS induced opposing changes in the expression levels of miR-3613-3p and MAP3K2 in HUVECs; however, whether miR-3613-3p directly or indirectly targets MAP3K2 remains unknown.

miR-3613-3p regulates the HS-induced apoptosis of HUVECs. To further understand the relationship between miR-3613-3p and the apoptosis of HS-exposed HUVECs, HUVECs were transfected with a miR-3613-3p inhibitor or miR-3613-3p mimic. Compared with the NC groups, cells successfully transfected with the miR-3613-3p inhibitor or miR-3613-3p mimic exhibited reduced or increased miR-3613-3p expression levels, respectively (Fig. 3A). HS significantly reduced the expression level of miR-3613-3p in HUVECs. The use of miR-3613-3p inhibitors further aggravated the reduction of miR-3613-3p in HUVECs exposed to HS. Moreover, the effect of miR-3613-3p inhibitor was dose-dependent, with the inhibition reaching its peak at 100 nM (Fig. 3B). The miR-3613-3p inhibitor, which led to a marked decrease in miR-3613-3p expression, resulted in upregulation of HS-induced apoptosis. The effects of the miR-3613-3p inhibitor were dose-dependent and peaked at 100 nM (Fig. 3C). Transfection of miR-3613-3p mimic could partially reverse the inhibition effect of HS on miR-3613-3p in HUVECs. The effect was dose-dependent, peaking at 50 nM (Fig. 3D). In addition, transfection with the miR-3613-3p mimic reduced HS-induced apoptosis of

HUVECs in a dose-dependent manner. This effect gradually increased with increasing miR-3613-3p mimic concentration and reached a peak at 50 nM (Fig. 3E). These results indicated a regulatory effect of miR-3613-3p on the HS-induced apoptosis of HUVECs. The similar effects of the miR-3613-3p mimic at 50 and 100 nM were considered to be related to the degree of saturation of intermediate binding sites between the miR-3613-3p mimic and mRNA. In subsequent experiments, the optimal concentration of 100 nM miR-3613-3p inhibitor or 50 nM miR-3613-3p mimic was used.

MAP3K2 is a target of miR-3613-3p in HUVECs. Previous bioinformatics analysis indicated that MAP3K2 may be a target gene of miR-3613-3p (12). The present study investigated the relationship between miR-3613-3p and MAP3K2 in the context of HS. Overexpression of miR-3613-3p in HUVECs induced using the miR-3613-3p mimic inhibited HS-induced MAP3K2 expression (Fig. 4A), whereas suppression of miR-3613-3p induced using the miR-3613-3p inhibitor enhanced HS-induced MAP3K2 expression in HUVECs (Fig. 4B). To further confirm whether the predicted target sites of miR-3613-3p were located within the 3'-UTR of MAP3K2 mRNA, dual luciferase reporter assays were performed with either the MAP3K2-WT or MAP3K2-MUT plasmid in HUVECs at 37°C. A schematic representation of the putative miR-3613-3p binding site in the MAP3K2 mRNA 3'-UTR is shown in Fig. 4C. Reduced luciferase activity was detected in HUVECs transfected with MAP3K2-WT and the miR-3613-3p mimic compared with that in HUVECs co-transfected with MAP3K2-WT and miR-NC (Fig. 4D). Moreover, the luciferase assay data indicated that luciferase activity was significantly increased in HUVECs co-transfected with MAP3K2-WT and

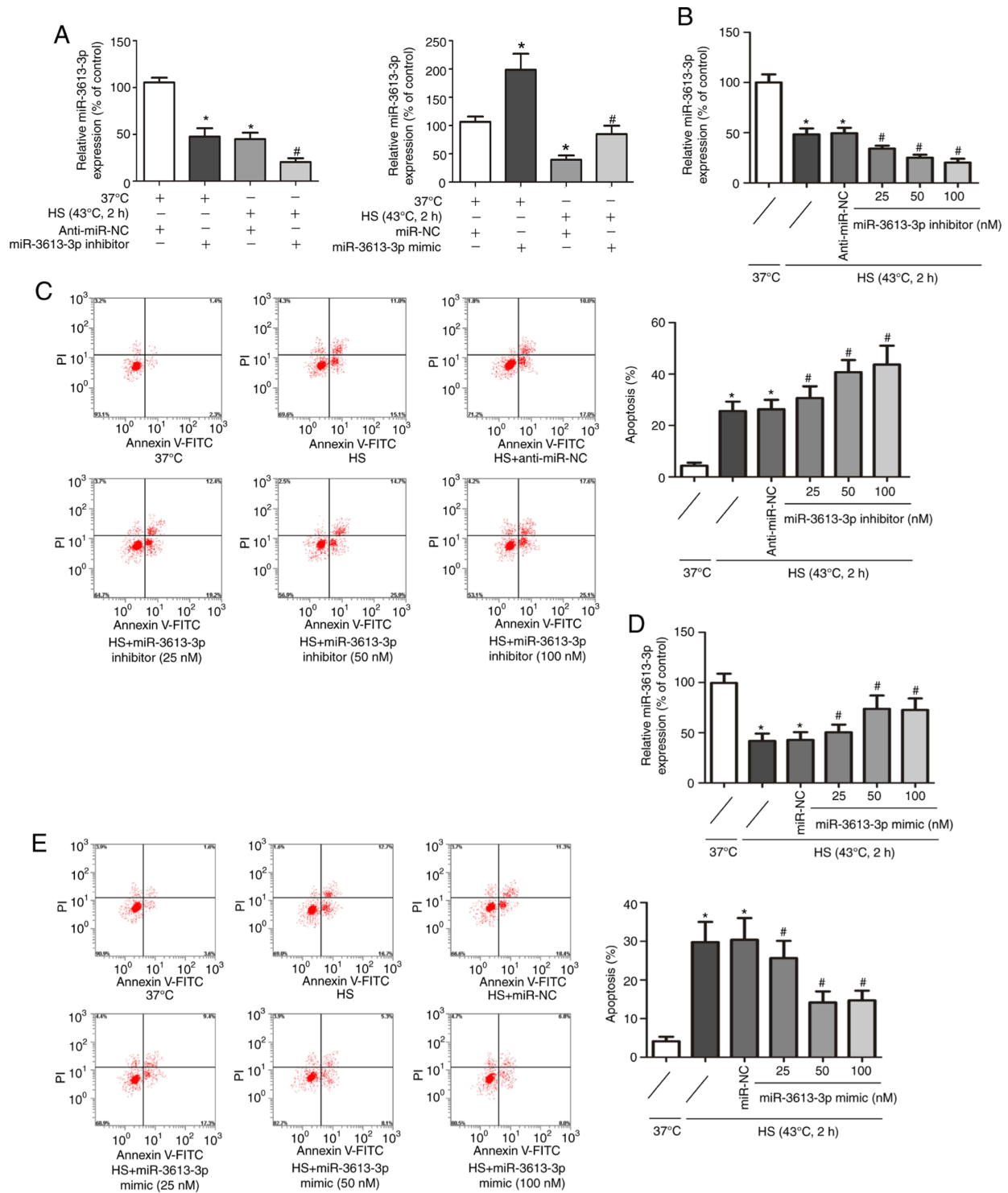


Figure 3. miR-3613-3p regulates the HS-induced apoptosis of HUVECs. (A) Reverse transcription-quantitative PCR analysis of miR-3613-3p expression in miR-3613-3p inhibitor- or miR-3613-3p mimic-transfected cells. * $P < 0.05$ vs. 37°C + anti-miR-NC/miR-NC group; # $P < 0.05$ vs. HS + anti-miR-NC/miR-NC group. (B) Expression of miR-3613-3p in HUVECs after HS exposure and/or miR-3613-3p silencing. * $P < 0.05$ vs. 37°C group; # $P < 0.05$ vs. HS + anti-miR-NC group. (C) Apoptosis of HUVECs after HS exposure and/or miR-3613-3p silencing. * $P < 0.05$ vs. 37°C group; # $P < 0.05$ vs. HS + anti-miR-NC group. (D) Expression of miR-3613-3p in HUVECs after HS exposure and/or miR-3613-3p overexpression. * $P < 0.05$ vs. 37°C group; # $P < 0.05$ vs. HS + miR-NC group. (E) Apoptosis of HUVECs after HS exposure and/or miR-3613-3p overexpression. * $P < 0.05$ vs. 37°C group; # $P < 0.05$ vs. HS + miR-NC group. FITC, fluorescein isothiocyanate; HUVECs, human umbilical vein endothelial cells; HS, heat stress; miR, microRNA; NC, negative control; PI, propidium iodide.

the miR-3613-3p inhibitor compared with that in HUVECs co-transfected with MAP3K2-WT and anti-miR-NC (Fig. 4E). Conversely, no change in the luciferase activity of the MAP3K2-MUT vector was detected after co-transfection with the miR-3613-3p mimic, the miR-3613-3p inhibitor or the

corresponding NC (Fig. 4D and E). Collectively, these data indicated that MAP3K2 was a target of miR-3613-3p.

MAP3K2 mediates HS-induced HUVEC apoptosis. The present study also aimed to determine whether MAP3K2 was involved in

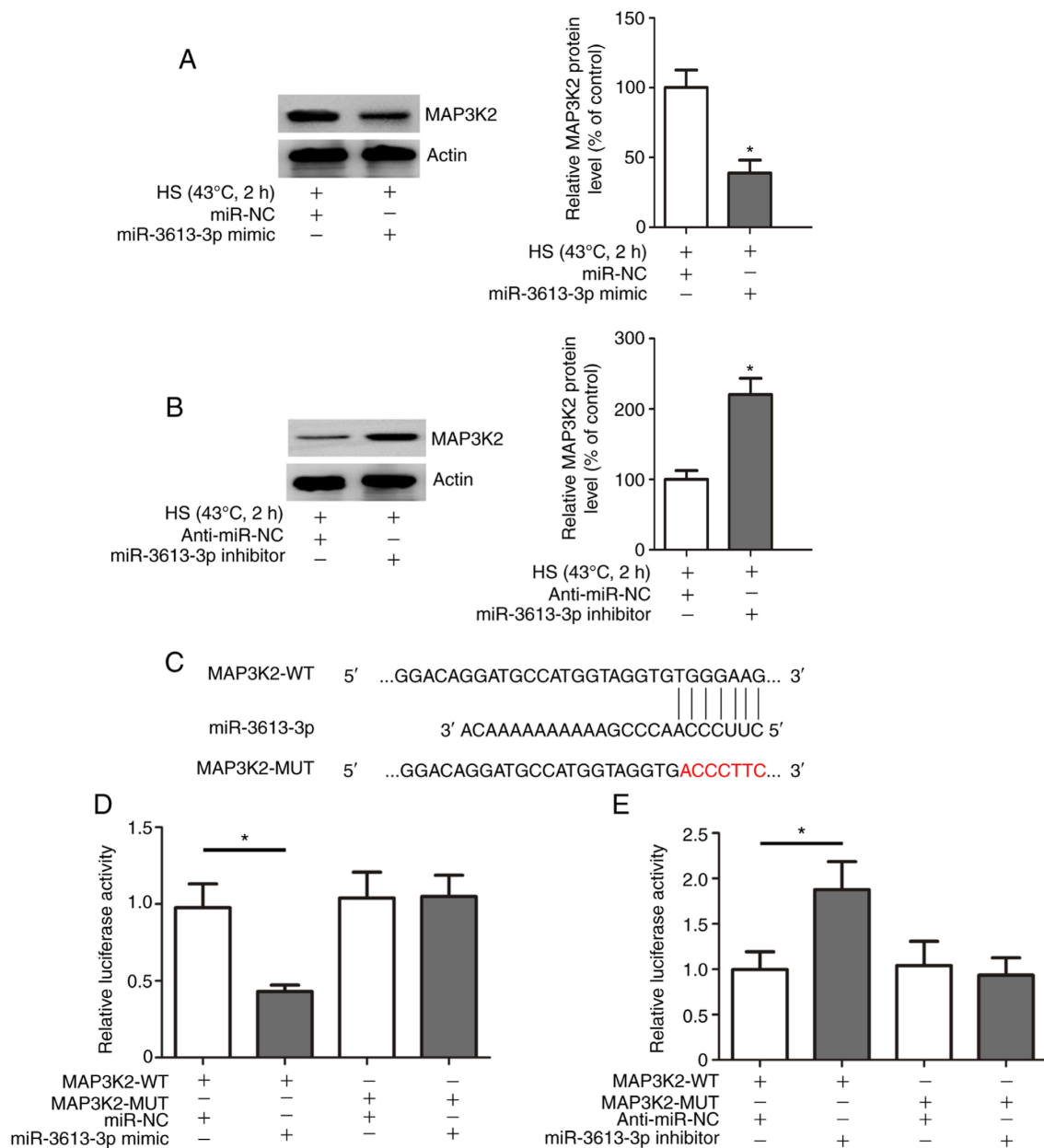


Figure 4. MAP3K2 is a target of miR-3613-3p in HUVECs. (A) Expression of MAP3K2 in HUVECs after HS exposure and/or miR-3613-3p overexpression. * $P < 0.05$ vs. HS + miR-NC group. (B) Expression of MAP3K2 in HUVECs after HS exposure and/or miR-3613-3p silencing. * $P < 0.05$ vs. HS + anti-miR-NC group. (C) Schematic representation of the putative miR-3613-3p binding site in the 3'-untranslated region of MAP3K2. MAP3K2-MUT indicates the MAP3K2 3'-UTR with a mutation in the miR-3613-3p binding site. (D) Relative luciferase activity in HUVECs after transfection with luciferase reporter plasmids (MAP3K2-WT or MAP3K2-MUT) and miR-3613-3p mimic or miR-NC was determined by a luciferase reporter assay. (E) Relative luciferase activity in HUVECs after transfection with luciferase reporter plasmids (MAP3K2-WT or MAP3K2-MUT) and miR-3613-3p inhibitor or anti-miR-NC was determined by a luciferase reporter assay. * $P < 0.05$, as indicated. HUVECs, human umbilical vein endothelial cells; HS, heat stress; MAP3K2, mitogen-activated protein kinase kinase kinase 3; miR, microRNA; MUT, mutant; NC, negative control; WT, wild type.

the HS-induced apoptosis of HUVECs. As shown in Fig. 5A and C, HUVECs were successfully transfected with si-MAP3K2 or pcDNA3.1-MAP3K2; compared with in the control groups, the transfected cells exhibited decreased or increased protein expression levels of MAP3K2, respectively. Notably, si-MAP3K2 treatment protected HUVECs from HS-induced apoptosis (Fig. 5B), whereas pcDNA3.1-MAP3K2 treatment resulted in increased HS-induced apoptosis of HUVECs (Fig. 5D).

miR-3613-3p acts through MAP3K2 to influence HUVEC apoptosis. To determine whether MAP3K2 was involved in

the pathogenic role of miR-3613-3p in HS-induced HUVEC apoptosis, the present study investigated the relationship among miR-3613-3p, MAP3K2 and apoptosis in HS-exposed HUVECs. MAP3K2 expression and apoptosis in HUVECs following HS were significantly inhibited by the miR-3613-3p mimic. Transfection with pcDNA3.1-MAP3K2 partially reversed the miR-3613-3p mimic-induced inhibition of MAP3K2 expression and apoptosis (Fig. 6A and B), whereas transfection with si-MAP3K2 promoted the miR-3613-3p mimic-induced inhibition of MAP3K2 expression and apoptosis (Fig. 6C and D).

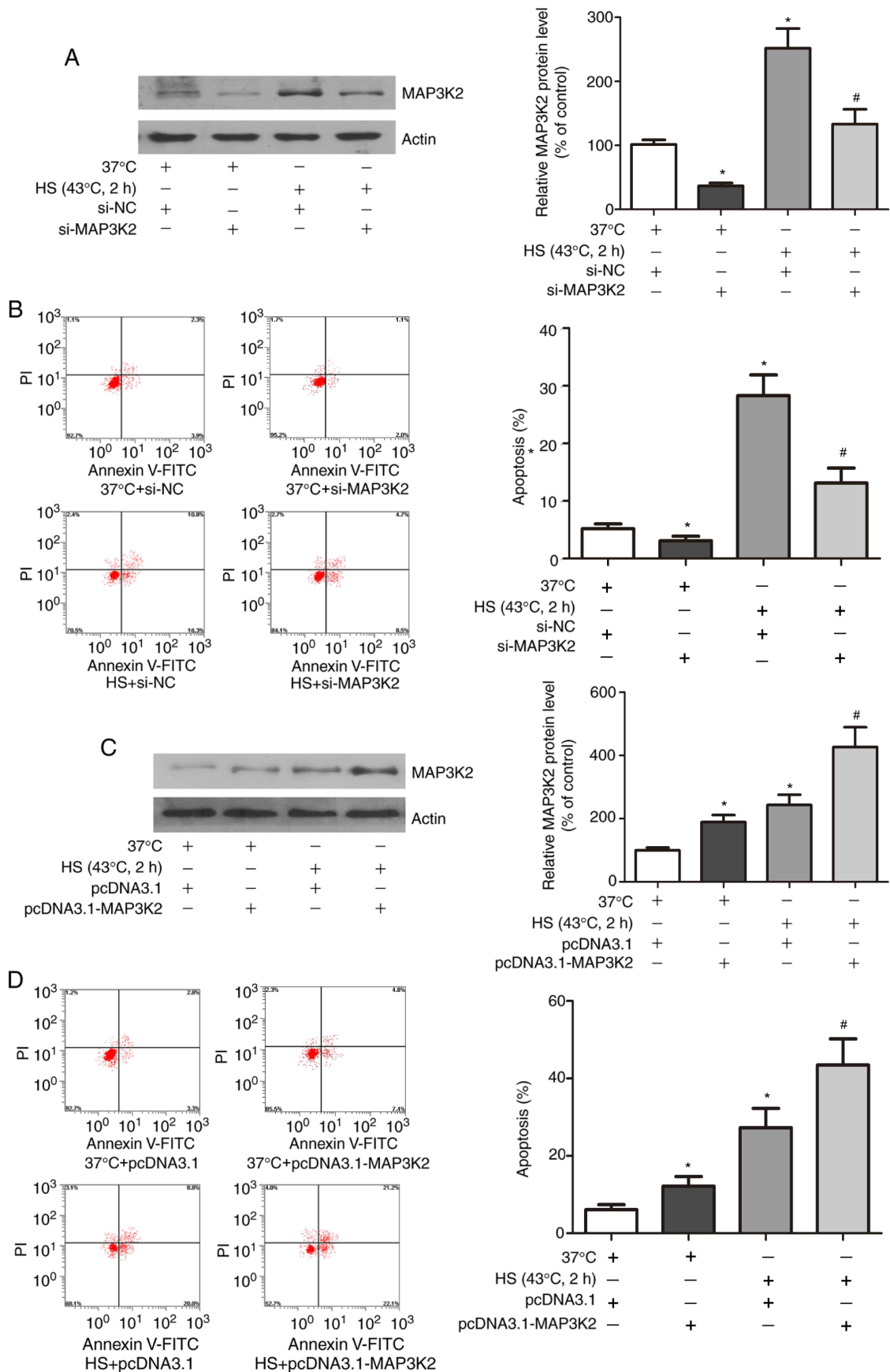


Figure 5. MAP3K2 mediates HS-induced HUVEC apoptosis. (A) Western blot analysis of MAP3K2 protein expression in si-MAP3K2- or si-NC-transfected cells. * $P < 0.05$ vs. 37°C + si-NC group; # $P < 0.05$ vs. HS + si-NC group. (B) Apoptosis of HUVECs after HS exposure and/or MAP3K2 silencing. * $P < 0.05$ vs. 37°C group; # $P < 0.05$ vs. HS group. (C) Western blot analysis of MAP3K2 protein expression in pcDNA3.1-MAP3K2- or pcDNA3.1-transfected cells. * $P < 0.05$ vs. 37°C group; # $P < 0.05$ vs. HS + pcDNA3.1 group. (D) Apoptosis of HUVECs after HS exposure and/or MAP3K2 overexpression. * $P < 0.05$ vs. 37°C + pcDNA3.1 group; # $P < 0.05$ vs. HS group. FITC, fluorescein isothiocyanate; HUVECs, human umbilical vein endothelial cells; HS, heat stress; MAP3K2, mitogen-activated protein kinase kinase kinase 3; miR, microRNA; NC, negative control; PI, propidium iodide; si, small interfering.

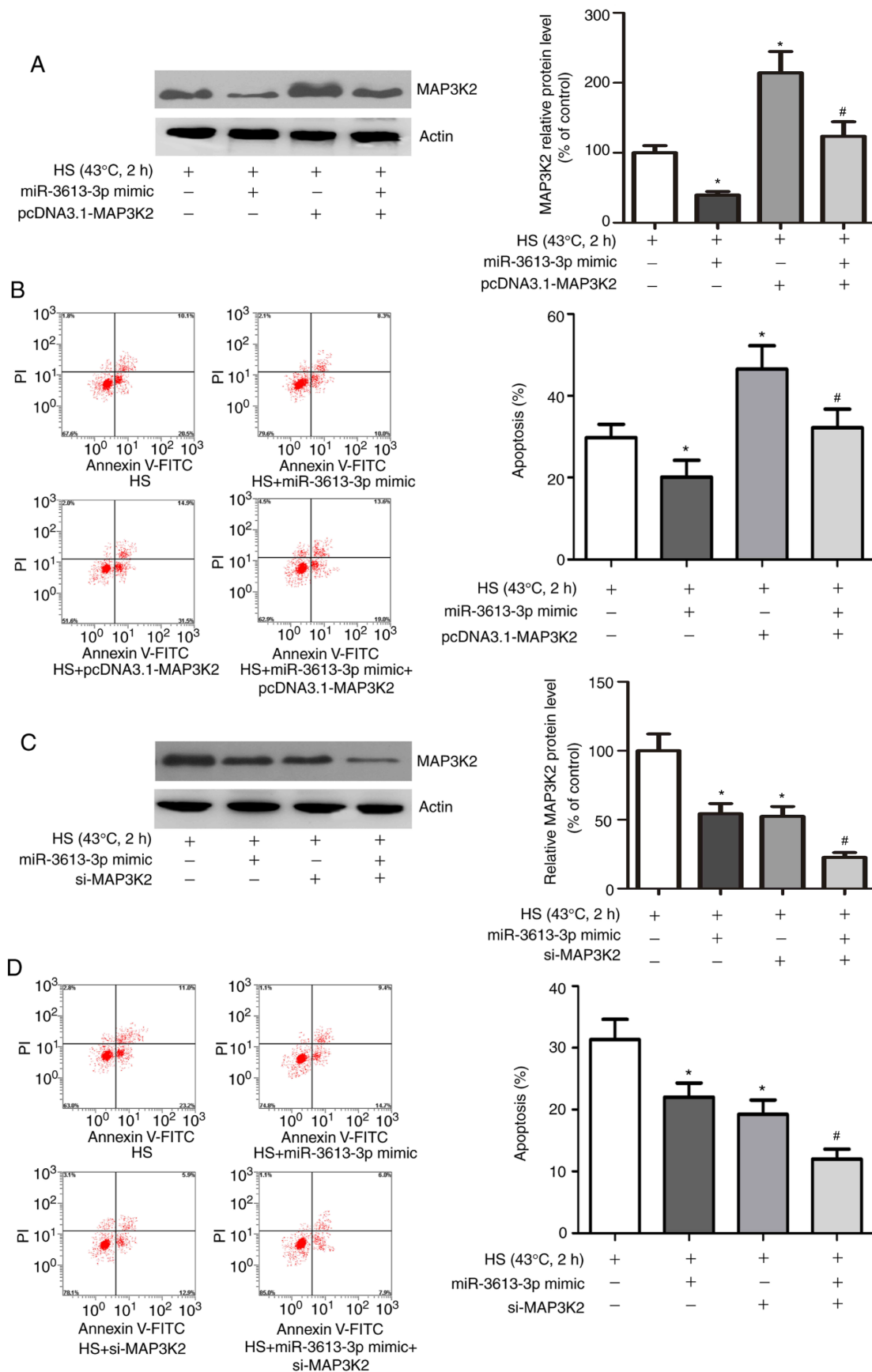


Figure 6. miR-3613-3p acts through MAP3K2 to influence HUVEC apoptosis. (A) Expression of MAP3K2 in HUVECs after HS exposure, miR-3613-3p overexpression and/or MAP3K2 overexpression. (B) Apoptosis of HUVECs after HS exposure, miR-3613-3p overexpression and/or MAP3K2 overexpression. (C) Expression of MAP3K2 in HUVECs after HS exposure, miR-3613-3p overexpression and/or silencing MAP3K2. (D) Apoptosis of HUVECs after HS exposure, miR-3613-3p overexpression and/or silencing MAP3K2. *P<0.05 vs. HS group; #P<0.05 vs. HS + miR-3613-3p mimic. FITC, fluorescein isothiocyanate; HUVECs, human umbilical vein endothelial cells; HS, heat stress; MAP3K2, mitogen-activated protein kinase kinase kinase 3; miR, microRNA; NC, negative control; PI, propidium iodide; si, small interfering.

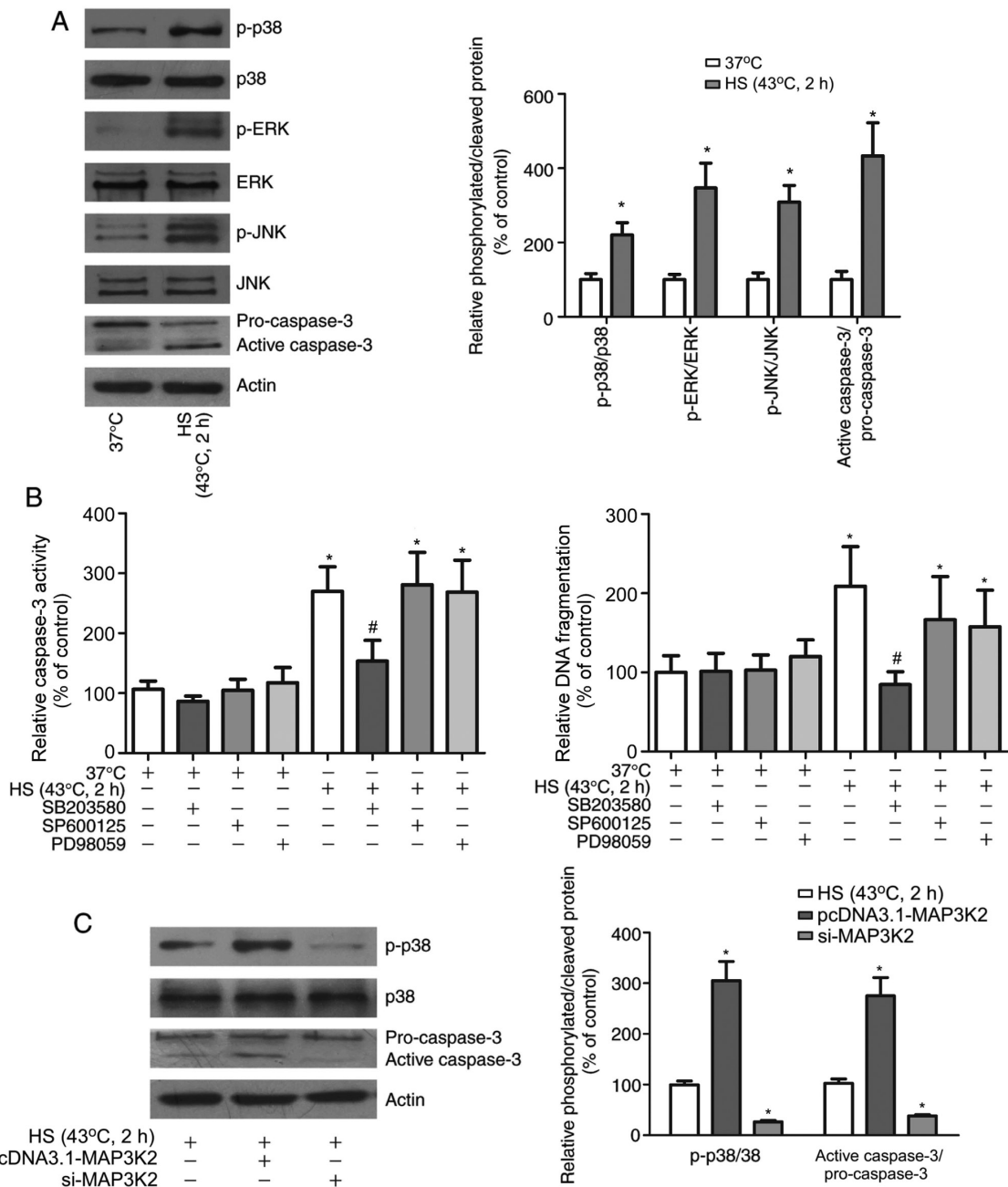


Figure 7. MAP3K2 affects the HS-induced apoptosis of HUVECs by upregulating p38 phosphorylation and caspase-3 activity. (A) Expression and phosphorylation of p38, ERK and JNK, and the level of cleaved caspase-3 in HUVECs after HS exposure. (B) Caspase-3 activity and DNA fragmentation in HUVECs after HS exposure and treatment with SB203580, SP600125 or PD98059. * $P < 0.05$ vs. 37°C group; # $P < 0.05$ vs. HS group. (C) Expression and phosphorylation of p38 and the level of cleaved caspase-3 in HUVECs after HS exposure and MAP3K2 overexpression or knockdown. * $P < 0.05$ vs. HS group. ERK, extracellular signal-regulated kinase; HUVECs, human umbilical vein endothelial cells; HS, heat stress; JNK, c-Jun N-terminal kinase; MAP3K2, mitogen-activated protein kinase kinase kinase 3; p-, phosphorylated; si, small interfering.

MAP3K2 affects the HS-induced apoptosis of HUVECs by increasing p38 phosphorylation and caspase-3 activity. To elucidate the molecular mechanisms by which MAP3K2 mediates HUVEC apoptosis, the underlying signalling pathways were assessed. As shown in Fig. 7A, HS had no effect on the expression levels of p38, JNK and ERK, but significantly upregulated their phosphorylation. Moreover, HS resulted in cleavage of caspase-3 in HUVECs. To further investigate the effects of different MAPKs on the HS-induced apoptosis of HUVECs, HUVECs were exposed to HS and treated with a range of specific inhibitors, including SB203580, PD98059

and SP600125. As shown in Fig. 7B, inhibition of p38 MAPK, but not ERK or JNK, diminished the production of cleaved caspase-3 and DNA fragments in HS-treated HUVECs. In addition, the relationship between MAP3K2 and p38 was determined. Western blot analysis revealed that HS increased the phosphorylation of p38 and activation of caspase-3; notably, knockdown of MAP3K2 expression significantly suppressed the HS-induced increases in p38 phosphorylation and caspase-3 activation, whereas overexpression of MAP3K2 markedly promoted these effects (Fig. 7C). Collectively, these findings indicated that MAP3K2 may accelerate HUVEC

apoptosis induced by HS via regulation of the p38/caspase-3 signalling pathway.

Discussion

Accumulating evidence has indicated that miRNA and miRNA-mediated regulatory networks serve a vital role in the onset and development of endothelial cell-related diseases and may represent therapeutic targets (23-25). Our previous miRNA expression profiling data in HUVECs indicated that miR-3613-3p may be a HS-related miRNA (12). Furthermore, using an *in vivo* approach, our previous study revealed a regulatory relationship between miR-3613-3p and MAP3K2 that mediated the apoptosis of HS-treated HUVECs (19).

The present study confirmed that miR-3613-3p could target MAP3K2 to suppress its protein expression and participate in HS-mediated HUVEC apoptosis. This conclusion was confirmed by the following experiments: i) A negative association between miR-3613-3p and MAP3K2 expression was observed in HUVECs upon exposure to HS. ii) Inhibition of miR-3613-3p promoted MAP3K2 expression, whereas upregulation of miR-3613-3p suppressed MAP3K2 expression. iii) miR-3613-3p negatively regulated MAP3K2 expression in HUVECs via binding to a site in the 3'-UTR of MAP3K2 mRNA. Notably, luciferase activity induced by the MAP3K2-WT plasmid was specifically responsive to miR-3613-3p, unlike the MAP3K2-MUT plasmid. iv) In a HS model, inhibition of MAP3K2 decreased HS-induced apoptosis, whereas HS-induced apoptosis was increased when MAP3K2 expression was enhanced. v) Restoration of MAP3K2 expression partially restored the suppression of apoptosis induced by miR-3613-3p overexpression, whereas inhibition of MAP3K2 enhanced miR-3613-3p-induced suppression of apoptosis. Thus, the present results indicated that MAP3K2 was a target of miR-3613-3p in terms of molecular mechanism and function.

There are three types of MAPK in the evolutionarily conserved MAPK cascades: MAPK kinase kinases (MAP3Ks), MAPK kinases (MAP2Ks) and MAPKs. By sequentially activating each other, MAPKs transduce signals from the activated receptors to the nucleus (26,27). MAP3K2 is an upstream kinase in the MAPK signalling pathway and has been reported to participate in numerous important cellular processes, such as apoptosis, proliferation and differentiation (28-30). To explore the biological function of MAP3K2 in the HS-induced apoptosis of HUVECs, the present study assessed the downstream genes of MAP3K2. HS stimulation increased ERK, JNK and p38 MAPK phosphorylation in HUVECs when apoptosis was notably increased, which was accompanied by increased cleavage of caspase-3. Moreover, inhibition of p38, but not JNK or ERK, markedly suppressed HS-induced production of cleaved caspase-3 (a key executor of apoptosis) and DNA fragmentation. In addition, in the present study, the HS-induced increases in p38 phosphorylation and caspase-3 activation in HUVECs were partially reversed by suppression of MAP3K2. Moreover, upregulation of MAP3K2 enhanced the HS-induced phosphorylation of p38 and activation of caspase-3 in HUVECs. The p38 MAPK pathway has been reported to enhance caspase-3 activity by promoting heat shock protein (Hsp)27-78 phosphorylation and

MAPK-activated protein kinase 2 (MK2) expression in neural stem cells (31). In nerve cells, targeting other oncogenes downstream of p38, such as Bcl-2-like protein 11, has been reported to increase caspase-3 activity (32). These findings collectively suggest that p38 may act as the downstream target of MAP3K2 and could promote apoptosis via caspase-3 in HUVECs upon exposure to HS.

p38 MAPK is first activated by typical MEKK or mixed-lineage kinases, then activates mitogen-activated protein kinase kinase 3 (MKK3) and MKK6, which are highly selective for p38 MAPK (33,34). In general, MAP3K2 phosphorylation was previously reported to preferentially regulate the JNK and ERK5 pathways by phosphorylating and activating MKK5 as well as MAP kinase 7 (35-38). However, the functional experiments in the present study revealed that HS-induced activation of the MAP3K2 pathway in a p38-dependent manner and resulted in HUVEC apoptosis. Consistent with the present findings, some previous studies have reported that MAP3K2 is associated with the activation of p38 (28,39). For example, sublytic C5b-9 promoted the apoptosis of glomerular mesangial cells by activating the MAP3K2/p38 MAPK axis (28). These findings indicated that the pathways engaged by MAP3K2 are highly context dependent, and vary by both cell type and stimulus.

Liu *et al* (40) observed that significant phosphorylation of p38 occurred in HUVECs after 15 min at 43°C. Li *et al* (41) investigated the time course of p38 MAPK phosphorylation in HUVECs stimulated by HS; p38 phosphorylation was detected as early as 1 h after heat shock and continued to the 9-h time point, which was also consistent with the time period during which caspase-9 and caspase-3 activation, Bcl-2 ubiquitination and apoptosis occurred. Similar to the alterations observed in HUVECs, p38 MAPK was shown to be rapidly activated after heat shock in glial cells; its phosphorylation peaked at 3 h and was maintained to the 12-h time point in glial cells, consistent with the time course of HS-induced apoptosis (42). Additionally, phosphorylation of p38 has been shown to be elevated at 6 h after HS in intestinal epithelial cells (43), and HS-induced activation of p38 was measurable in cardiomyocytes 1 h after HS exposure (44). In this study, phosphorylation of p38 was at a high level 2 h after HS, coinciding with the decrease in miR-3613-3p and increase in MAP3K2 expression. p38 MAPK is a downstream molecule of multiple signalling pathways, and is eventually activated through signalling pathways composed of extracellular signalling molecules, specific receptors on the surface of the membrane and intracellular signalling molecules (45-47). Notably, the initiation time and duration of p38 MAPK activation are irregular and may vary with different cell types or environmental stresses.

In addition to the present findings, previous studies have revealed that HS can activate different MAPK signalling pathways in a variety of cell types. p-MAPKs, which are downstream genes of MAPKs, and some of their downstream molecules, were the focus of these studies. Li *et al* (31) indicated that p38/MK2/Hsp27-78 signalling was activated during HS-induced apoptosis and autophagy progression in neural stem cell. In addition, Liu *et al* (44) reported that HS promoted the activation of p38, leading to cardiomyocyte apoptosis and cardiac dysfunction. Huang *et al* (15) indicated that the ERK pathways participated in the HS-induced receptor-interacting

protein 1/3-dependent necroptosis of pulmonary vascular endothelial cells, which exacerbated lung injury. A previous study also indicated that activation of p38/c-Jun served a proapoptotic role in HS-induced intestinal epithelial cell apoptosis, which eventually led to reduced epithelial barrier integrity and increased intestinal permeability, whereas ERK conferred resistance to apoptosis (43). In summary, these data suggested that both the activation of MAPKs and the biological outcome of MAPK activation are dependent on the intensity/duration of HS and are cell type- and tissue-specific. However, the relationship between HS and MAPK signalling is complex, and whether a single MAPK pathway drives functions in various physiological processes, or whether the same physiological process involves multiple MAPK pathways requires further research.

Some limitations of the current study must be mentioned: i) The present study used HUVECs to reveal the mechanism underlying HS-induced apoptosis. All experiments were in cell models, which may have major differences from *in vivo* models and cannot perfectly imitate the clinical course of HS. Future *in vivo* studies are required to determine the effect of endothelial cell apoptosis on heat-related organ dysfunction. ii) Endothelial cells in different organs may exhibit different responses to HS due to differences in organ function and the local internal environment, although the organ specificity of endothelial cells was not considered in the present study. iii) miRNA and signalling pathways are connected by complex interactions and regulatory mechanisms that form positive and/or negative regulatory networks. The effects of other miRNA molecules and signalling pathways were not considered. iv) Although SB203580 has been widely used in previous studies to inhibit protein, siRNA can inhibit protein production as they directly inhibit mRNA. In future studies, siRNA targeting p38 will be used to obtain improved results.

In conclusion, the present study revealed that HS induced HUVEC apoptosis via regulation of the miR-3613-3p/MAP3K2/p38/caspase-3 axis. The present findings also provided insight into the role of miR-3613-3p during heat stroke, suggesting the modulation of miR-3613-3p as a potential therapeutic strategy for heat stroke.

Acknowledgements

The authors would like to thank Dr Qiping Lu (Department of General Surgery, Central Theater General Hospital of the People's Liberation Army of China, Wuhan, China) for her advice and Dr Guoguo Zhu (Department of Emergency, Central Theater General Hospital of the People's Liberation Army of China, Wuhan, China) for her help in preparing the manuscript.

Funding

No funding was received.

Availability of data and materials

The datasets used and/or analysed during the current study are available from the corresponding author on reasonable request.

Authors' contributions

JL participated in the design of the study, carried out experiments and data analysis, performed drafting and editing of the manuscript, and was a major contributor to the writing of the manuscript. SX and SL participated in the experiments, data analysis and statistical analysis. BC conceived and designed the experiments, edited and revised the manuscript, and approved the final version of the manuscript. All authors read and approved the final manuscript. JL and BC confirm the authenticity of all the raw data.

Ethics approval and consent to participate

Ethical approval was obtained for the use of non-immortal HUVECs from the Ethics Committee of Hefei Boe Hospital Co., Ltd. (approval no. 20190106).

Patient consent for publication

Not applicable.

Competing interests

The authors declare that they have no competing interests.

References

- Jin H, Chen Y, Ding C, Lin Y, Chen Y, Jiang D and Su L: Microcirculatory disorders and protective role of Xuebijing in severe heat stroke. *Sci Rep* 8: 4553, 2018.
- Bouchama A and Knochel JP: Heat stroke. *N Engl J Med* 346: 1978-1988, 2002.
- Roberts GT, Ghebeh H, Chishti MA, Al-Mohanna F, El-Sayed R, Al-Mohanna F and Bouchama A: Microvascular injury, thrombosis, inflammation, and apoptosis in the pathogenesis of heatstroke: A study in baboon model. *Arterioscler Thromb Vasc Biol* 28: 1130-1136, 2008.
- Lam NN, Hung TD and Hung DK: Acute respiratory distress syndrome among severe burn patients in a developing country: Application result of the berlin definition. *Ann Burns Fire Disasters* 31: 9-12, 2018.
- Haines RJ, Wang CY, Yang CGY, Eitnier RA, Wang F and Wu MH: Targeting palmitoyl acyltransferase ZDHHC21 improves gut epithelial barrier dysfunction resulting from burn-induced systemic inflammation. *Am J Physiol Gastrointest Liver Physiol* 313: G549-G557, 2017.
- Bouchama A, Hammami MM, Haq A, Jackson J and al-Sedairy S: Evidence for endothelial cell activation/injury in heatstroke. *Crit Care Med* 24: 1173-1178, 1996.
- Oshima K, Han X, Ouyang Y, El Masri R, Yang Y, Haeger SM, McMurtry SA, Lane TC, Davizon-Castillo P, Zhang F, *et al*: Loss of endothelial sulfatase-1 after experimental sepsis attenuates subsequent pulmonary inflammatory responses. *Am J Physiol Lung Cell Mol Physiol* 317: L667-L677, 2019.
- Colbert JF and Schmidt EP: Endothelial and microcirculatory function and dysfunction in sepsis. *Clin Chest Med* 37: 263-275, 2016.
- Bombeli T, Mueller M and Haerberli A: Anticoagulant properties of the vascular endothelium. *Thromb Haemost* 77: 408-423, 1997.
- Donadello K, Piagnerelli M, Reggiori G, Gottin L, Scolletta S, Occhipinti G, Zouaoui Boudjeltia K and Vincent JL: Reduced red blood cell deformability over time is associated with a poor outcome in septic patients. *Microvasc Res* 101: 8-14, 2015.
- Bartel DP: MicroRNAs: Genomics, biogenesis, mechanism, and function. *Cell* 116: 281-297, 2004.
- Liu J, Zhu G, Xu S, Liu S, Lu Q and Tang Z: Analysis of miRNA expression profiling in human umbilical vein endothelial cells affected by heat stress. *Int J Mol Med* 40: 1719-1730, 2017.

13. Corre I, Paris F and Huot J: The p38 pathway, a major pleiotropic cascade that transduces stress and metastatic signals in endothelial cells. *Oncotarget* 8: 55684-55714, 2017.
14. Li M, van Esch BCAM, Wagenaar GTM, Garssen J, Folkerts G and Henricks PAJ: Pro- and anti-inflammatory effects of short chain fatty acids on immune and endothelial cells. *Eur J Pharmacol* 831: 52-59, 2018.
15. Huang W, Xie W, Gong J, Wang W, Cai S, Huang Q, Chen Z and Liu Y: Heat stress induces RIP1/RIP3-dependent necroptosis through the MAPK, NF- κ B, and c-Jun signaling pathways in pulmonary vascular endothelial cells. *Biochem Biophys Res Commun* 528: 206-212, 2020.
16. Yong YX, Yang H, Lian J, Xu XW, Han K, Hu MY, Wang HC and Zhou LM: Up-regulated microRNA-199b-3p represses the apoptosis of cerebral microvascular endothelial cells in ischemic stroke through down-regulation of MAPK/ERK/EGR1 axis. *Cell Cycle* 18: 1868-1881, 2019.
17. Zhou Z, Chen Y, Zhang D, Wu S, Liu T, Cai G and Qin S: MicroRNA-30-3p suppresses inflammatory factor-induced endothelial cell injury by targeting TCF21. *Mediators Inflamm* 2019: 1342190, 2019.
18. Yi J and Gao ZF: MicroRNA-9-5p promotes angiogenesis but inhibits apoptosis and inflammation of high glucose-induced injury in human umbilical vascular endothelial cells by targeting CXCR4. *Int J Biol Macromol* 130: 1-9, 2019.
19. Liu J, Han X, Zhu G, Liu S, Lu Q and Tang Z: Analysis of potential functional significance of microRNA-3613-3p in human umbilical vein endothelial cells affected by heat stress. *Mol Med Rep* 20: 1846-1856, 2019.
20. Tang S, Allagadda V, Chibli H, Nadeau JL and Mayer GD: Comparison of cytotoxicity and expression of metal regulatory genes in zebrafish (*Danio rerio*) liver cells exposed to cadmium sulfate, zinc sulfate and quantum dots. *Metallomics* 5: 1411-1422, 2013.
21. Tang S, Cai Q, Chibli H, Allagadda V, Nadeau JL and Mayer GD: Cadmium sulfate and CdTe-quantum dots alter DNA repair in zebrafish (*Danio rerio*) liver cells. *Toxicol Appl Pharmacol* 272: 443-452, 2013.
22. Livak KJ and Schmittgen TD: Analysis of relative gene expression data using real-time quantitative PCR and the 2(-Delta Delta C(T)) method. *Methods* 25: 402-408, 2001.
23. Li X, Xue X, Sun Y, Chen L, Zhao T, Yang W, Chen Y and Zhang Z: MicroRNA-326-5p enhances therapeutic potential of endothelial progenitor cells for myocardial infarction. *Stem Cell Res Ther* 10: 323, 2019.
24. Xing X, Li Z, Yang X, Li M, Liu C, Pang Y, Zhang L, Li X, Liu G and Xiao Y: Adipose-derived mesenchymal stem cells-derived exosome-mediated microRNA-342-5p protects endothelial cells against atherosclerosis. *Aging (Albany NY)* 12: 3880-3898, 2020.
25. Deng X, Chu X, Wang P, Ma X, Wei C, Sun C, Yang J and Li Y: MicroRNA-29a-3p reduces TNF α -induced endothelial dysfunction by targeting tumor necrosis factor receptor 1. *Mol Ther Nucleic Acids* 18: 903-915, 2019.
26. Zehorai E and Seger R: Beta-like importins mediate the nuclear translocation of mitogen-activated protein kinases. *Mol Cell Biol* 34: 259-270, 2014.
27. Lee Y, Kim YJ, Kim MH and Kwak JM: MAPK cascades in guard cell signal transduction. *Front Plant Sci* 7: 80, 2016.
28. Zhu G, Qiu W, Li Y, Zhao C, He F, Zhou M, Wang L, Zhao D, Lu Y, Zhang J, *et al*: Sublytic C5b-9 induces glomerular mesangial cell apoptosis through the cascade pathway of MEKK2-p38 MAPK-IRF-1-TRADD-caspase 8 in rat Thy-1 nephritis. *J Immunol* 198: 1104-1118, 2017.
29. Chen Z, Zhu R, Zheng J, Chen C, Huang C, Ma J, Xu C, Zhai W and Zheng J: Cryptotanshinone inhibits proliferation yet induces apoptosis by suppressing STAT3 signals in renal cell carcinoma. *Oncotarget* 8: 50023-50033, 2017.
30. Chang X, Liu F, Wang X, Lin A, Zhao H and Su B: The kinases MEKK2 and MEKK3 regulate transforming growth factor- β -mediated helper T cell differentiation. *Immunity* 34: 201-212, 2011.
31. Li H, Liu Y, Wen M, Zhao F, Zhao Z, Liu Y, Lin X and Wang L: Hydroxysafflor yellow A (HSYA) alleviates apoptosis and autophagy of neural stem cells induced by heat stress via p38 MAPK/MK2/Hsp27-78 signaling pathway. *Biomed Pharmacother* 114: 108815, 2019.
32. Zhuang Y, Xu H, Richard SA, Cao J, Li H, Shen H, Yu Z, Zhang J, Wang Z, Li X and Chen G: Inhibition of EPAC2 attenuates intracerebral hemorrhage-induced secondary brain injury via the p38/BIM/caspase-3 pathway. *J Mol Neurosci* 67: 353-363, 2019.
33. Barata AG and Dick TP: A role for peroxiredoxins in H₂O₂- and MEKK-dependent activation of the p38 signaling pathway. *Redox Biol* 28: 101340, 2020.
34. Deschodt-Lanckman M and Strosberg AD: In vitro degradation of the C-terminal octapeptide of cholecystokinin by 'enkephalinase A'. *FEBS Lett* 152: 109-113, 1983.
35. Dermott JM, Ha JH, Lee CH and Dhanasekaran N: Differential regulation of Jun N-terminal kinase and p38MAP kinase by Galphal2. *Oncogene* 23: 226-232, 2004.
36. Raviv Z, Kalie E and Seger R: MEK5 and ERK5 are localized in the nuclei of resting as well as stimulated cells, while MEKK2 translocates from the cytosol to the nucleus upon stimulation. *J Cell Sci* 117: 1773-1784, 2004.
37. Shen CT, Qiu ZL, Song HJ, Wei WJ and Luo QY: miRNA-106a directly targeting RARB associates with the expression of Na(+)/I(-) symporter in thyroid cancer by regulating MAPK signaling pathway. *J Exp Clin Cancer Res* 35: 101, 2016.
38. Tsioumpekou M, Papadopoulos N, Burovic F, Heldin CH and Lennartsson J: Platelet-derived growth factor (PDGF)-induced activation of Erk5 MAP-kinase is dependent on Mek2, Mek1/2, PKC and PI3-kinase, and affects BMP signaling. *Cell Signal* 28: 1422-1431, 2016.
39. Shi X, Liu TT, Yu XN, Balakrishnan A, Zhu HR, Guo HY, Zhang GC, Bilegsaikhan E, Sun JL, Song GQ, *et al*: microRNA-93-5p promotes hepatocellular carcinoma progression via a microRNA-93-5p/MAP3K2/c-Jun positive feedback circuit. *Oncogene* 39: 5768-5781, 2020.
40. Liu Y, Zhou G, Wang Z, Guo X, Xu Q, Huang Q and Su L: NF- κ B signaling is essential for resistance to heat stress-induced early stage apoptosis in human umbilical vein endothelial cells. *Sci Rep* 5: 13547, 2015.
41. Li L, Tan H, Yang H, Li F, He X, Gu Z, Zhao M and Su L: Reactive oxygen species mediate heat stress-induced apoptosis via ERK dephosphorylation and Bcl-2 ubiquitination in human umbilical vein endothelial cells. *Oncotarget* 8: 12902-12916, 2017.
42. Li H, Liu Y, Gu Z, Li L, Liu Y, Wang L and Su L: p38 MAPK-MK2 pathway regulates the heat-stress-induced accumulation of reactive oxygen species that mediates apoptotic cell death in glial cells. *Oncol Lett* 15: 775-782, 2018.
43. Liu Y, Wang Z, Xie W, Gu Z, Xu Q and Su L: Oxidative stress regulates mitogen-activated protein kinases and c-Jun activation involved in heat stress and lipopolysaccharide-induced intestinal epithelial cell apoptosis. *Mol Med Rep* 16: 2579-2587, 2017.
44. Liu ZF, Ji JJ, Zheng D, Su L and Peng T: Calpain-2 protects against heat stress-induced cardiomyocyte apoptosis and heart dysfunction by blocking p38 mitogen-activated protein kinase activation. *J Cell Physiol* 234: 10761-10770, 2019.
45. Pu Y, Liu Z, Tian H and Bao Y: The immunomodulatory effect of Poria cocos polysaccharides is mediated by the Ca²⁺/PKC/p38/NF- κ B signaling pathway in macrophages. *Int Immunopharmacol* 72: 252-257, 2019.
46. Wang W, Weng J, Yu L, Huang Q, Jiang Y and Guo X: Role of TLR4-p38 MAPK-Hsp27 signal pathway in LPS-induced pulmonary epithelial hyperpermeability. *BMC Pulm Med* 18: 178, 2018.
47. Zhang X, Chen Q, Song H, Jiang W, Xie S, Huang J and Kang G: MicroRNA-375 prevents TGF- β -dependent transdifferentiation of lung fibroblasts via the MAP2K6/P38 pathway. *Mol Med Rep* 22: 1803-1810, 2020.



This work is licensed under a Creative Commons Attribution-NonCommercial-NoDerivatives 4.0 International (CC BY-NC-ND 4.0) License.